JOURNAL OF SOLID STATE CHEMISTRY 72, 283–292 (1988)

Vibrational Study of Metal-Substituted MPS_3 Layered Compounds: $M^{II}_{1-x}M^{I}_{2x}PS_3$ with M^{II} = Mn, Cd, and M^{I} = Cu (x = 0.13) or Ag (x = 0.50)

II. Low-Frequency Raman Study and Ionic Transport

O. POIZAT* AND F. FILLAUX

LASIR, CNRS, 2 rue Henri Dunant, 94320 Thiais, France

AND C. SOURISSEAU

Laboratoire de Spectroscopie Moléculaire et Cristalline, UA 124, CNRS, Université de Bordeaux I, 33405 Talence, France

Received February 18, 1987

The low-frequency Raman spectra of $Mn_{0.87}Cu_{0.26}PS_3$, $Cd_{0.87}Cu_{0.26}PS_3$, $Mn_{0.5}Ag_{1.0}PS_3$, and $Cd_{0.5}Ag_{1.0}PS_3$ layered compounds have been recorded from powder samples and/or single crystals between 15 and 800 K. The temperature dependences of these spectra reflect the dynamics of the M^I ions and they have been fitted using different theoretical models. In $Mn_{0.87}Cu_{0.26}PS_3$ a nonlinear coupling between the Cu^I translational mode perpendicular to the layer plane and an intralayer vibration governs the passage of the copper ions into the interlayer space, which is a determining step in the ionic conductivity process. Similar conductivity properties are expected in $Cd_{0.87}Cu_{0.26}PS_3$. In contrast, this step is not observed in the silver-containing compounds.

Introduction

In this paper we discuss the dynamic properties of the title compounds over the temperature range 15 to 800 K. Recently, ionic conductivity properties have been found in some $M^{II}_{1-x}M^{I}_{2x}PX_3$ derivatives (with X = S, Se) and ascribed to mobility of the M^I ions. In particular, Gulbinski and Feltz (*1*) have shown the existence of silver transport and conductivity in $Cd_{1-x}Ag_{2x}PSe_3$ compounds ($0 \leq x \leq 0.15$). Similarly, in $Mn_{0.87}Cu_{0.26}PS_3$ we have characterized (*2*) a weak but strongly temperature-dependent ionic conductivity. The increase, between 300 and 600 K, of the conductivity parallel to the layer plane by four orders of magnitude suggests the existence of a thermally activated transport process, and preliminary Raman spectra obtained (*2*) from powder samples between 125 and 450 K have revealed unexpected temperature variations of the bands ascribed to Cu^I translational modes.

To better understand the cation dynamics in this class of compounds, new Raman studies of $Mn_{0.87}Cu_{0.26}PS_3$, $Cd_{0.87}Cu_{0.26}PS_3$, $Mn_{0.5}Ag_{1.0}PS_3$, and $Cd_{0.5}Ag_{1.0}PS_3$ powders and single crystals were carried out between 15 and 800 K. Complete vibrational assignments were already proposed in a previous paper (*3*); here, we discuss the very low frequency region (0–100 cm^{-1}) where translational modes of the copper and silver cations appear.

* To whom correspondence should be addressed.

0022-4596/88 $3.00

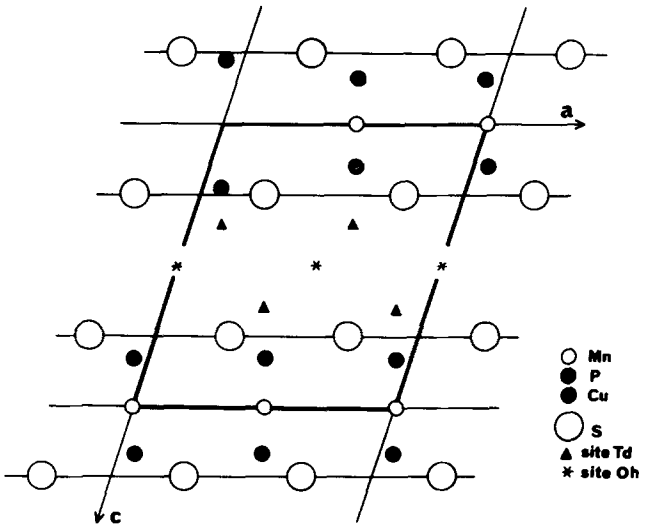

FIG. 1. Schematic representation of the projection of the $Mn_{0.87}Cu_{0.26}PS_3$ structure in the a, c directions.

Experimental

Sample preparation and handling have been described in Part I (*3*). Raman spectra were recorded with a triple monochromator Dilor RTI30 instrument equipped with a Spectra Physics SP164 argon ion laser (λ_0 = 514.5 nm). Efficient rejection of the incident interference light at ± 5 cm^{-1} above the excitation laser line was performed with a homemade monochromator. Detection was carried out using a cooled RCA C31023 photomultiplier tube and rapid scans were accumulated in a microcomputer controlling the spectrometer. Low-temperature spectra (15–300 K) were obtained with a liquid helium cryostat (Meric) and high-temperature measurements (300–800 K) were performed using a homemade furnace (*4*). Temperature effects have been demonstrated on powder samples for all compounds and on single crystals for $Mn_{0.87}Cu_{0.26}PS_3$ and $Cd_{0.87}Cu_{0.26}PS_3$.

Results

The crystal structure of $Mn_{0.87}Cu_{0.26}PS_3$ (Fig. 1) has been determined by Mathey *et al.* (*5*). Layers developed in the $a \times b$ directions, composed of juxtaposed P_2S_6, MnS_6, and S_3Cu . . . CuS_3 pseudooctahedra, are separated by van der Waals gaps. The Cu^I ions are located inside the layers at ca. 0.14 Å from the sulfur plane. The structures of the other compounds are not known but probably can be compared (*3*) to that of $Mn_{0.87}Cu_{0.26}PS_3$.

The low-frequency Raman signals assigned to translational modes of the M^I ions are strongly temperature dependent (Figs. 2–4), whereas the rest of the spectra remain essentially unchanged.

For the Cu^I intercalated single-crystal platelets in the (ZZ) configuration, the low-frequency Raman bands near 60 and 45 cm^{-1} (Figs. 2 and 3) are ascribed to copper translational components along a coordinate (T'_z) perpendicular to the layer plane (*3*). The intensity of the high-frequency signal (ν_0) vanishes at high temperature, while the intensity of the low-frequency component (ν_1) increases rapidly above 300 K. Simultaneously, frequencies and bandwidths are but little affected. These effects most probably reflect the dynamics of the Cu^I

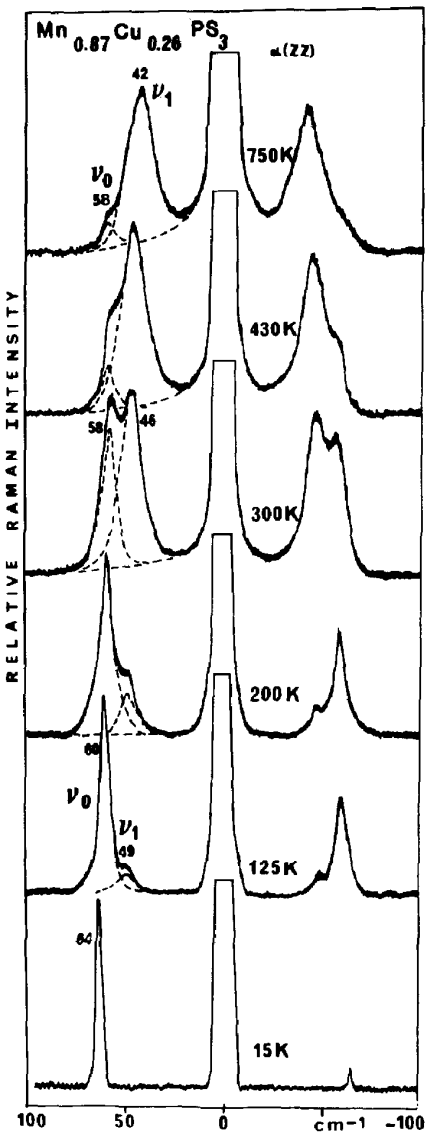

FIG. 2. Raman spectra (−100 to +100 cm^{-1}) of a monocrystalline $Mn_{0.87}Cu_{0.26}PS_3$ platelet (α_{zz} configuration) between 15 and 750 K.

ions along the T'_z coordinate, and since there is no evidence from the rest of the spectra for significant structural transition, a thermally activated jumping mechanism is likely to take place.

The low-frequency spectra of the silver-containing compounds (Fig. 4) show three peaks near 22, 31, and 48 cm^{-1} at 300 K, corresponding to T'_{xy}, T'_z, and T'_{xy} Ag^I vibrations (*3*). Larger bandwidths and band splittings observed at low temperature for $Mn_{0.5}Ag_{1.0}PS_3$ may be due to superstructure effects (*6*). For both compounds, the main bands show similar temperature effects which differ from those observed for the copper derivatives: intensities increase continuously from 25 to 750 K and there is no relative intensity inversion.

The mean amplitudes of the M^I ions in the z direction can be estimated from the T'_z frequencies, in the harmonic approximation, by using the Cruickshank equation (*7*):

$$\langle u_z^2(M^I)\rangle = \frac{h}{8\pi^2 cm\nu(T'_z)} \coth \frac{hc\nu(T'_z)}{2kT}. \quad (1)$$

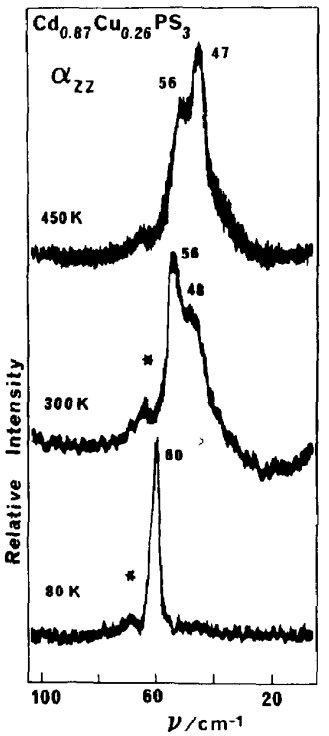

FIG. 3. Raman spectra (0–100 cm^{-1}) of a $Cd_{0.87}Cu_{0.26}PS_3$ monocrystalline platelet (α_{zz} configuration) between 80 and 450 K.

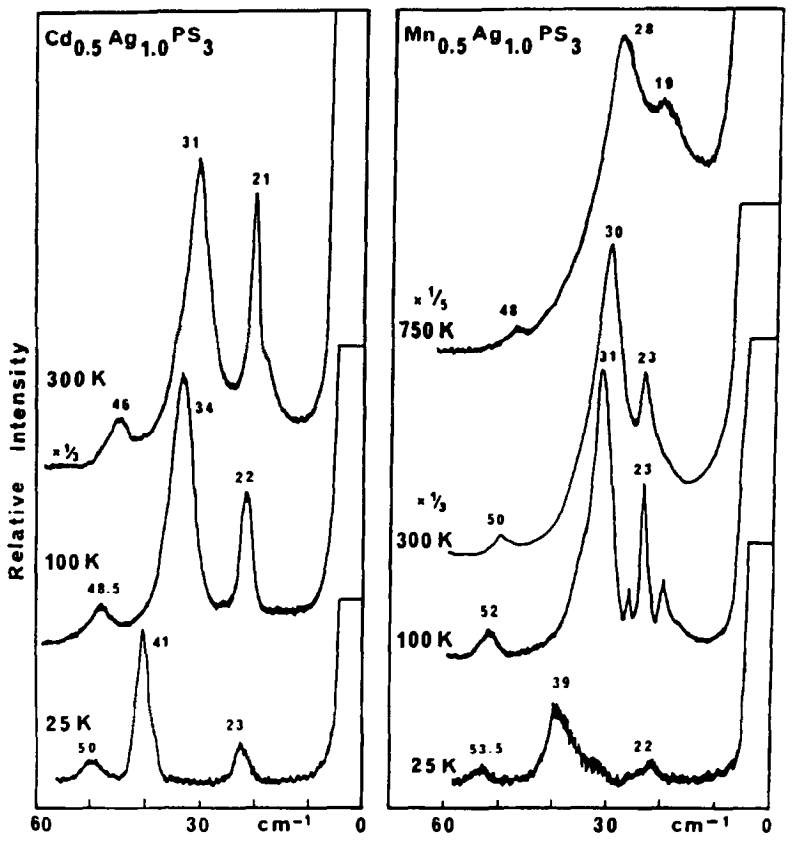

FIG. 4. Raman spectra (0–60 cm^{-1}) of $Cd_{0.5}Ag_{1.0}PS_3$ (left) and $Mn_{0.5}Ag_{1.0}PS_3$ (right) polycrystalline samples between 25 and 750 K.

The values found at 300 and 750 K are reported in Table I. The copper oscillation amplitude in $Mn_{0.87}Cu_{0.26}PS_3$ at 300 K (low-temperature state) agrees with that determined from XRD thermal factors (5) ($\langle u_z^2 \rangle^{1/2}$ = 0.13 Å). Very large vibrational amplitudes are observed at high temperature in all cases. This is consistent with the existence of very large $(M^I)_2S_6$ octahedra in these structures.

Temperature effects suggest that Cu^I and Ag^I dynamics are not the same. The Cu^I motion is certainly different at low and high temperatures and one may assume either a double minimum potential along T_z' or two different potentials linked by another translational coordinate or a nonlinear coupling

TABLE I

BAND WAVENUMBERS $\nu(T_z')$ AND MEAN T_z' AMPLITUDES OF THE Cu^I IONS IN THEIR LOW-TEMPERATURE (L.T.) AND HIGH-TEMPERATURE (H.T.) STATES AND OF THE Ag^I IONS IN THE $M^{II}_{1-x}M^I_{2x}PS_3$ COMPOUNDS (M^{II} = Mn, Cd)

	$M^{II}_{0.87}Cu^I_{0.26}PS_3$		
	L.T. state (ν_0)	H.T. state (ν_1)	$M^{II}_{0.5}Ag^I_{1.0}PS_3$
300 K			
$\nu(T_z')$	58 cm^{-1}	46 cm^{-1}	30 cm^{-1}
$\langle u_z^2 \rangle^{1/2}$	0.17 Å	0.22 Å	0.25 Å
750 K			
$\nu(T_z')$	58 cm^{-1}	42 cm^{-1}	28 cm^{-1}
$\langle u_z^2 \rangle^{1/2}$	0.27 Å	0.34 Å	0.35 Å

with an internal mode in the layer. In the next part a quantitative analysis of the data shows that the last assumption is the most satisfactory. Contrarily, there is no evidence for multiple Ag^I sites in the silver-containing compounds and temperature effects may be explained accordingly.

Theoretical Models and Discussions

The dynamics of the cations can be described in terms of potential functions consistent with the observed frequency and intensity variations with temperature. This is possible since, owing to their very low frequencies, many vibrational states of the T_z' modes are rapidly occupied when the temperature increases and the observed effects are related to the anharmonicity (i.e., the shape) of the potential experienced by the cations.

The basic assumption of the model is that, within their T_z' potentials, the Cu^I and Ag^I ions jump randomly between the ground and excited states, dividing their time in the ratio of the Boltzmann population factors, and the jumping rate is so rapid that only the thermally averaged frequencies and intensities are observed. Similar hypotheses have been widely used to account for the large temperature effects observed for very low frequency methyl torsional modes (*8–12*). Considering the first-order transition moment, the observed frequency for an oscillator is

$$\nu(T) = \frac{1}{h}\frac{\sum_0^N [(n+1)/D\nu(n)][E(n+1) - E(n)]\exp[-E(n)/RT]}{\sum_0^N [(n+1)/D\nu(n)]\exp[-E(n)/RT] + RT\exp(-Eb/RT)} \tag{2}$$

N is the number of discrete levels and $D\nu(n)$ represents the bandwidth for the $n \rightarrow n+1$ transition. The last term in the denominator accounts for the continuum above the threshold energy Eb corresponding to a possible escape of the cation from its site. The bandwidth may vary to a large extent and probably increases rapidly for higher excited states. When it is large enough, the contribution of the corresponding transition to the observed band is embedded in the spectral baseline and may be neglected. In this case, a simplified approach is to consider only the lowest $K+1$ levels of the oscillator:

$$\nu(T) = \frac{1}{h}\frac{\sum_0^K (n+1)[E(n+1) - E(n)]\exp[-E(n)/RT]}{\sum_0^K (n+1)\exp[-E(n)/RT]} \tag{3}$$

The number K has no real physical meaning since it represents only an equivalent number of equally damped vibrational levels and it provides a poor phenomenological estimate of the unknown variation of the damping with the energy of the state.

For the Ag^I-containing compounds, the intensities of the T' bands increase rapidly and continuously much in the same way as expected for a harmonic oscillator (frequency ν_0) with negligible damping factor variations:

$$I(T) = \alpha\frac{\sum_0^\infty (n+1)\exp(-nh\nu_0/RT)}{\sum_0^\infty \exp(-nh\nu_0/RT)} \tag{4}$$

or

$$I(T) = \alpha\frac{1}{1 - \exp(-h\nu_0/RT)}. \tag{5}$$

Here α is proportional to the square of the

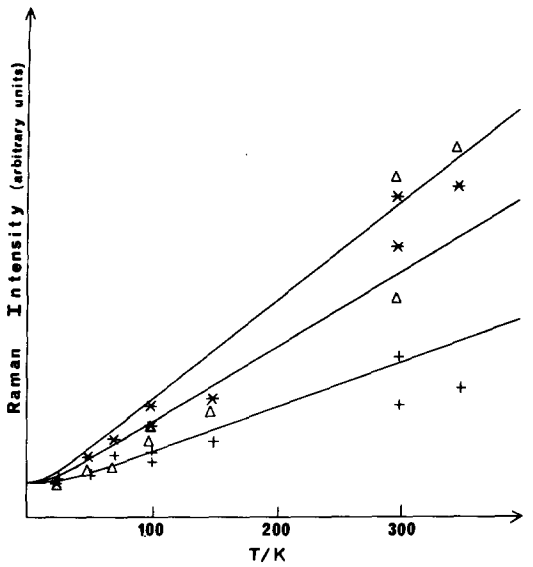

FIG. 5. Temperature effect on the intensity of the $T'(Ag^I)$ modes in $Mn_{0.5}Ag_{1.0}PS_3$: experimental data for the components at 23 cm^{-1} (*), 30 cm^{-1} (△), and 50 cm^{-1} (+) and calculated curves for harmonic potentials.

transition moment. The temperature effect is determined entirely by the frequency of the mode and this model accounts qualitatively for the different intensity enhancements for the two compounds at high temperature. Figure 5 shows the experimental and calculated temperature dependences of the intensities of the $T'(Ag)$ modes in $Mn_{0.5}Ag_{1.0}PS_3$. Very similar plots are obtained with $Cd_{0.5}Ag_{1.0}PS_3$. Discrepancies between observed and calculated intensities may be due to the effects of anharmonicity and damping of the upper vibrational states which have been neglected. There is no evidence for contributions that could be ascribed to a continuum and the energy threshold is certainly very high.

For the copper-containing compounds, owing to thermal averaging, a double minimum potential along T'_z is unlikely. Therefore, each band is ascribed to an anharmonic potential which remains unchanged at any temperature. Temperature effects on frequencies thus reflect the anharmonicity of each potential while relative intensity variations are governed by two simultaneous factors: the variation of intensity inside each potential and the relative occupation probabilities.

The lowest energy levels are supposed to fulfill the equation

$$E(n+1) - E(n) = E(n) - E(n-1) - nDE \quad (6)$$

which describes the anharmonicity near the minimum. The relation may not hold for the whole potential and the dissociation threshold (Eb), if it exists, is considered an independently adjustable parameter.

The averaged integrated intensity for each potential ($j = 0$ and 1 corresponding to the high- and low-frequency components, respectively) is

$$I_j(T) = \alpha_j \frac{\sum_0^K (n+1)\exp[-E(n)/RT]}{\sum_0^N \exp[-E(n)/RT] + RT\exp(-Eb/RT)} \quad (7)$$

with K much lower than the maximum number of discrete levels according to Eq. (6). α_j is proportional to the square of the transition moment for the T'_z mode.

If the two bands are ascribed to two different sites for the Cu^I ions separated by a potential barrier E along another translational coordinate, the intensities for the high- and low-frequency components are determined by the Boltzmann occupation probability factors of a two-state system:

$$J_0(T) = \frac{1}{1+\exp(-E/RT)} I_0(T) \quad (8)$$

$$J_1(T) = \frac{\exp(-E/RT)}{1+\exp(-E/RT)} I_1(T) \quad (9)$$

Alternatively, it may be supposed that there is a nonlinear coupling of T'_z to a mode

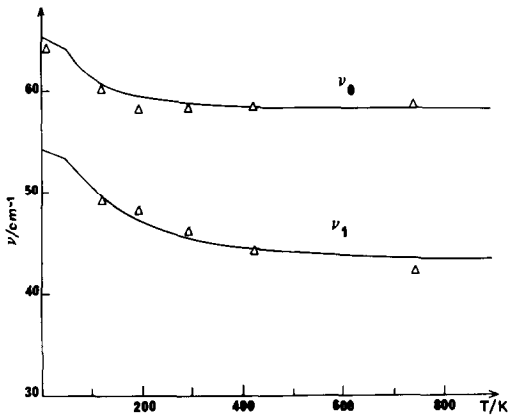

FIG. 6. Temperature dependence of the $T_z'(Cu^I)$ frequencies in $Mn_{0.87}Cu_{0.26}PS_3$: experimental data (△) and calculated curves (—) for the ν_0 component, with E_0 = 65 cm^{-1}, DE = 4 cm^{-1}, and K = 4 (upper trace), and for the ν_1 component, with E_0 = 54 cm^{-1}, DE = 2 cm^{-1}, and K = 11 (lower trace). E_0, DE, and K are the $0 \rightarrow 1$ transition energy, the anharmonic increment, and the number of levels, respectively.

of the layer lattice: the band at very low temperature (ν_0) then corresponds to the Cu^I dynamics when the layer mode is in its ground state, while the low-frequency band (ν_1) appears only when the layer mode is in its first excited state. Assuming a harmonic potential of frequency ν_X for the layer mode, the corresponding intensities are then

$$J_0(T) = [1 - \exp(-h\nu_X/RT)]I_0(T) \quad (10)$$

$$J_1(T) = \exp(-h\nu_X/RT)\,[1 - \exp(-h\nu_X/RT)]I_1(T). \quad (11)$$

The formulas are slightly different if all the excited states of the X mode are supposed to contribute to the low-frequency component:

$$J_0(T) = [1 - \exp(-h\nu_X/RT)]I_0(T) \quad (12)$$

$$J_1(T) = [\exp(-h\nu_X/RT)]I_1(T). \quad (13)$$

The parameters included in the different models have been adjusted to fit the observed frequency (Fig. 6) and intensity variations (Fig. 7 and Table II) for $Mn_{0.87}Cu_{0.26}PS_3$. All values, being more or less model dependent, deserve serious reserve and must be considered as only indicative; however, it appears that some reliable information concerning the dynamics of the Cu^I ions at different temperatures may be sorted out.

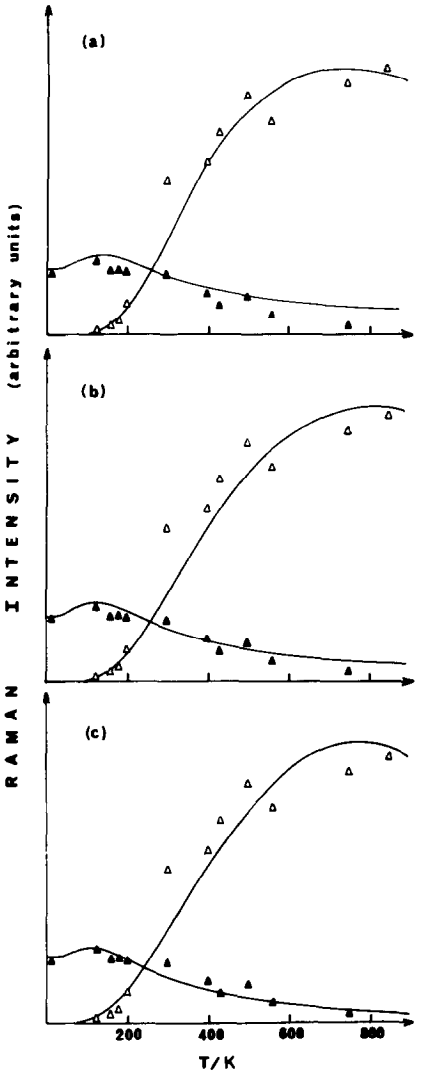

FIG. 7. Temperature effects on the intensity of the $T_z'(Cu^I)$ components in $Mn_{0.87}Cu_{0.26}PS_3$. (▲) Experimental data for the high-frequency component (ν_0), (△) experimental data for the low-frequency component (ν_1), (—) curves calculated with the parameters shown in Table II for models a, b, and c, respectively.

TABLE II

PARAMETER VALUES DERIVED FROM TEMPERATURE EFFECTS ON THE INTENSITY OF THE $T'_z Cu^I$ BANDS NEAR 60 AND 45 cm^{-1}

	E_0	DE	K	α	Eb
Model a					
$P_0(T) = \frac{1}{1 + e^{-500h/RT}}$	65	4	3	1	undet.
$P_1(T) = \frac{e^{-500h/RT}}{1 + e^{-500h/RT}}$	54	2	25	160	4000
Model b					
$P_0(T) = 1 - e^{-350h/RT}$	65	4	3	1	undet.
$P_1(T) = e^{-350h/RT}[1 - e^{-350h/RT}]$	54	2	25	1.8	4000
Model c					
$P_0(T) = 1 - e^{-250h/RT}$	65	4	3	1	undet.
$P_1(T) = e^{-250h/RT}$	54	2	22	1	3000

Note. E_0 is the $0 \rightarrow 1$ transition, DE the anharmonic increment, K the number of energy levels, α the relative transition moments, and Eb the dissociation threshold. Frequencies and energies are in cm^{-1}. Models a, b, and c correspond to Eqs. (8) and (9), (10) and (11), and (12) and (13), respectively, in the text.

The frequency shifts depend only on the anharmonicity of the potentials and on the damping of the energy levels (or the equivalent number K), but not on the activation process for the high-temperature regime. It appears that only a very limited number of energy levels (3 or 4) contribute to the high-frequency component near 60 cm^{-1}, whereas more than 10 levels must be included to fit the observed data for the low-frequency band. It is thus likely that the damping increases much more rapidly in the former than in the latter potential.

Owing to the large number of unknowns, the three models may account for the observed temperature effects on frequencies. The main uncertainty is the change in the Raman transition moment for the two potentials; however, it seems unlikely that this change exceeds one order of magnitude and thus the first model [Eqs. (8) and (9)], which requires the transition moment to vary by a factor of 160 (see Table II), is rejected. Therefore, the thermally activated process corresponds more probably to a nonlinear coupling of the T'_z mode to a lattice motion located in the region 250–340 cm^{-1}, i.e., a mode involving a deformation X of the PS_3 groups (*3*) ($\nu_s PS_3$, δPS_3 or $T'_{xy} PS_3$). This is consistent with the fact that from a structural point of view, the Cu^I ions are interacting with the sulfur atoms (*5*). This interaction is stronger in the fundamental than in the excited $X(PS_3)$ states and thus leads to a higher frequency, a lower oscillation amplitude, and a more rapidly increasing damping effect for the T'_z mode in the former state than in the latter states. Since no vibrational progression is observed for any mode in the region 250–350 cm^{-1}, even at high temperature, a significant shift of the T'_z potential minimum in the excited states is unlikely and the copper ions probably stay in their intralamellar sites. The dissociation threshold along the T'_z coordinate (3500 ± 500 $cm^{-1} \equiv$ 10.0 ± 1.4 kcal/mole) corresponds to Cu^I exiting from these sites. Since the half oscillation amplitude of Cu^I at 750 K ($1/2\ \langle u_z^2 \rangle^{1/2}$ = 0.17 Å; see Table I) is comparable to the dis-

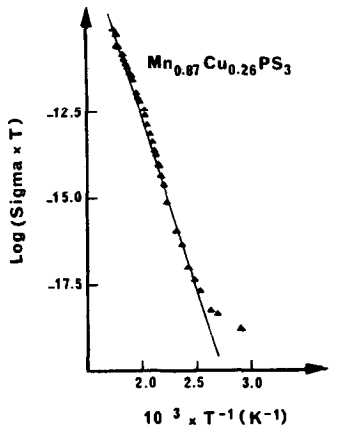

FIG. 8. Variation of the conductivity of $Mn_{0.87}Cu_{0.26}PS_3$ versus reciprocal temperature (▲) (the straight line corresponds to the Arrhenius plot obtained with $\Delta E_{activation} \sim 20$ kcal/mole).

tance between the intralamellar cation site and the sulfur layer (0.14 Å), the T'_z dissociation threshold can be identified with the energy barrier that the Cu^I ions must overcome to move from the layer to the van der Waals gap (Fig. 1). This energy limit is much lower than the activation energy (ΔE_a ~20 ± 3 kcal/mole) estimated from the slope of the conductivity curve (Fig. 8). This indicates that the ionic conductivity is only partially limited by the passage of the Cu^I ions into the interlamellar space where higher jumping barriers to free diffusion are encountered. Under these conditions the thermally controlled population of the $X(PS_3)$ states may be seen as a preliminary step of the complicated path along which the Cu^I ions trapped in the layer sites may enter the van der Waals gap and contribute to the ionic conductivity. Evidently, the participation of the $X(PS_3)$ mode in this mechanism reflects the fact that the sulfur atoms must move aside to allow the copper ions to enter the gap.

Although incomplete and poor-quality spectra do not justify performing theoretical calculations in the case of $Cd_{0.87}Cu_{0.26}PS_3$, temperature effects very similar to those reported for $Mn_{0.87}Cu_{0.26}PS_3$ are observed (Fig. 3) and the Cu^I dynamics is probably nearly the same in these compounds. In particular, a quantitatively comparable coupling of the $T'_z(Cu^I)$ mode with a PS_3 vibration near 250 cm^{-1} can be assumed in both cases. This is consistent with the fact that the $\nu(PS_3)$, $\delta(PS_3)$, and $T'_{xy}(PS_3)$ modes have nearly equal frequencies in $Mn_{0.87}Cu_{0.26}PS_3$ and in $Cd_{0.87}Cu_{0.26}PS_2$ (*3*). Similar ionic conductivity properties can thus be expected in these two lattices.

On the contrary, though the large Ag^I ions undergo very large amplitude T'_z motions and are obviously strongly interacting with the sulfur atoms, the $T'_z(Ag^I)$ potential remains essentially insensitive to excitations of the lattice modes and there is no spectroscopic evidence for dissociation threshold. No jumping or diffusion processes are seen, probably because of the large size of the silver cation. As a consequence, no ionic conductivity is expected in the silver-containing compounds within the temperature range considered.

Conclusion

The Cu^I translational modes in $Mn_{0.87}Cu_{0.26}PS_3$ and $Cd_{0.87}Cu_{0.26}PS_3$ are identified unambiguously from polarized Raman spectra on single crystals. The T'_z mode perpendicular to the layers is characterized by two bands having relative intensities strongly dependent upon temperature, and the Cu^I dynamics is not the same at low (~15 K) and high (>300 K) temperatures.

A quantitative analysis of the frequencies and intensities suggests that this change in dynamics may be due to a nonlinear coupling of the T'_z and a PS_3 internal mode near 250 cm^{-1}. Moreover, the energy threshold for the Cu^I ion to move from its intralayer site to the van der Waals gap is found in the range 3000–4000 cm^{-1}. The ionic conduc-

tivity in these compounds, resulting from Cu^I transport in the van der Waals gap, occurs probably via a complicated path which has not been completely explained; however, a first step in this process is the excitation of the PS_3 mode and the passage of the Cu^I ions into the interlamellar space. The activation energy derived from conductivity measurements ($\Delta E_a = 7000 \pm 1000$ cm^{-1}) shows that there are certainly additional potential barriers and energy dissipation processes on the way of the mobile cations.

No ionic transport is observed in the related silver-containing systems where the Ag^I ions are trapped in deep quasi-harmonic potentials. This is well explained by considering the large ionic volume and steric hindrance of Ag^I compared with Cu^I.

References

1. W. B. Gulbinski and A. Feltz, *Solid State Ionics* **20,** 159 (1986).
2. Y. Mathey, R. Clement, J. P. Audiere, O. Poizat, and C. Sourisseau, *Solid State Ionics* **9/10**, 459 (1983).
3. O. Poizat, C. Sourisseau, and Y. Mathey, *J. Solid State Chem.* **72,** 3961 (1988).
4. O. Poizat, thesis, Université Paris 6 (1985).
5. Y. Mathey, A. Michalowicz, P. Toffoli, and G. Vlaic, *Inorg. Chem.* **23,** 897 (1984).
6. W. G. McMullan and J. C. Irwin, *Canad. J. Phys.* **62,** 789 (1984).
7. D. W. J. Cruickshank, *Acta Crystallogr.* **9,** 1005 (1956).
8. S. C. Clough, *J. Phys. C* **9,** 1523 (1976); **14,** 1009 (1981).
9. A. C. Hawson, *J. Phys. C* **15,** 3841 (1982).
10. M. Punkkinen, *Phys. Rev. B* **21,** 54 (1980).
11. A. Huller, *Z. Phys. B* **36,** 215 (1980).
12. N. Le Calve, B. Pasquier, G. Braathen, L. Soulard, and F. Fillaux, *J. Phys. C* **19,** 6695 (1986).